Dalton Transactions

View Online
Dynamic Article Links

Cite this: DOI: 10.1039/c1dt10362h

www.rsc.org/dalton

PAPER

A versatile water soluble fluorescent probe for ratiometric sensing of Hg^{2+} and bovine serum albumin†

Jinghan Wen, Zhirong Geng, Yuxin Yin and Zhilin Wang*

Received 3rd March 2011, Accepted 11th July 2011
DOI: 10.1039/c1dt10362h

A novel tetraazamacrocycle fluorescent sensor (6-(1-(dimethylamino)-5-naphthalene sulfonyl)-3,6,9,15-tetraazabicyclo[9.3.1] pentadeca-1(15),11,13-triene, **1**) has been designed and prepared, which can be utilized for selective and ratiometric sensing of Hg^{2+} and bovine serum albumin (BSA) with two different responsive modes in aqueous solution at physiological pH (50 mM Tris-HCl, pH 7.6). Above 0.5 ppb Hg^{2+} can be discerned by coordination with **1** and the emission color changes enable **1** to be applied to a fast Hg^{2+} test paper assay. Sensor **1** has also been demonstrated to be easily cell-penetrable and applicable for Hg^{2+} imaging in living cells. Imaging of BSA in the gel using SDS-PAGE (sodium dodecyl sulfate polyacrylamide gel electrophoresis) stained in the medium containing **1** verified that the binding of **1** and BSA was successful in the presence of nonprotein substances. The linear range of **1** towards BSA utilizing ratiometric fluorescent calibration *via* noncovalent interaction in solution is 0–100 μg mL^{-1} with a detection limit of 1 μg mL^{-1}, and has been successfully employed to determine the albumin concentration in blood serum by means of ratiometric fluorescent measurements for the first time. Finally, sensor **1** behaves as a fluorescent molecular switch composed of triple logic gates upon chemical inputs of Hg^{2+} and BSA, which potentially provides intelligent diagnostics for Hg^{2+} contaminated serum on the nanoscale.

Introduction

Mercury(II), which is considered to be extremely hazardous among the metal cations, leads to severe digestive, kidney and neurological diseases[1] even at fairly low concentrations. Traditional quantitative approaches to determine Hg^{2+} employ analytical techniques including cold vapour atomic absorption spectrometry, cold vapour atomic fluorescence spectrometry, X-ray fluorescence spectrometry, inductively coupled plasma-mass spectrometry and voltammetry. Nevertheless, these methods often require complicated multistep sample preparation and/or sophisticated instrumentation.[2] Therefore, more recently, the exploration of sensitive and selective chemosensors for Hg^{2+} in both environmental and biological systems has been greatly stimulated.[3] To date, a number of Hg^{2+} detecting methods, including colorimetric and fluorescent strategies,[4] have been thoroughly examined. However, most of these sensors respond to Hg^{2+} merely by a change in the fluorescence intensity, which may be disturbed by the surrounding environment. On the contrary, ratiometric fluorescent sensors will be independent of environmental disturbance by calculating the ratio of the fluorescent intensities at two different wavelengths.[4i,4k,5] Besides, there are only a few examples of ratiometric fluorescent sensors for Hg^{2+}, especially in pure aqueous solution,[6] due to the poor water solubility of many fluorophores, providing opportunities to remedy this deficiency by designing novel ones.

On the other hand, serum albumin is well known to be the most abundant plasma protein in mammals, acting as a plasma carrier by moving many small molecules through the blood, including bilirubin, calcium, progesterone, and medications.[7] The relative lack of albumin may indicate liver and kidney diseases, or malnutrition owing to a low protein diet. Contrarily, severe or chronic dehydration has been verified to be associated with an excess of albumin.[8] Thus, it has been of great interest to utilize fluorescent sensors to determine the concentration of albumin in blood serum.[9] Similarly, ratiometric fluorescent sensors are preferred due to the capability of cancelling interferences in the complicated physiological media.

Moreover, tetraazamacrocycles cyclen[10] (1,4,7,10-tetraazacyclododecane) and cyclam[3a,11] (1,4,8,11-tetraazacyclotetradecane) derivatives have been reported to be able to coordinate strongly with Hg^{2+}. And when a dansyl (1-(dimethylamino)-5-naphthalenesulfonyl) group is covalently bound to a host molecule, it shows characteristic photophysical properties[12] and high sensitivity to the polarity of the medium.[13] Thereby motivated, we herein design and employ an analogous compound **L** (3,6,9,15-tetrazabicyclo[9.3.1]pentadeca-1(15),11,13-triene) as the dansyl fluorophore appended frame. The obtained macrocycle **1** exhibits

State Key Laboratory of Coordination Chemistry, Coordination Chemistry Institute, School of Chemistry and Chemical Engineering, Nanjing University, Nanjing, 210093, P. R. China. E-mail: wangzl@nju.edu.cn

† Electronic supplementary information (ESI) available: Characterization of **1**, binding behaviors of **1** towards Hg^{2+} and BSA, program describing the logic gates using C language, computationally optimized energies and coordinates of **1** and **1**-Hg^{2+}. See DOI: 10.1039/c1dt10362h

dual fluorescent responsive modes for both Hg^{2+} and bovine serum albumin (BSA). Sensor **1** shows high selectivity and sensitivity for ratiometric recognition of Hg^{2+} above 0.5 ppb in aqueous solution at physiological pH. And **1** has not only been successfully applied to a fast Hg^{2+} test paper assay, but is also demonstrated to be cell-permeable and able to visualize Hg^{2+} in living cells by utilizing inverted fluorescence microscopy. Besides, BSA could be detected by **1** at least down to 1 μg mL^{-1} *via* noncovalent interaction, which draws more attention[9d–e,14] because of the relatively facile and low-cost manipulations compared to the covalent-labeling method. More attractively, the binding of **1** and BSA has been verified to be unaffected in the presence of nonprotein substances when **1** was exploited to stain BSA after electrophoresis using 1-D SDS-PAGE (sodium dodecyl sulfate polyacrylamide gel electrophoresis) gels. BSA concentration could also be determined in blood serum by means of ratiometric fluorescent measurements using **1**.

Furthermore, the fluorescent response of **1** at different wavelengths towards various inputs not only allows for ratiometric fluorescent measurements, but also enables us to employ it as a fluorescent molecular switch composed of multiple logic gates. Silicon-based logic gates have been widely applied to computers, communications and circuits with Boolean calculations such as AND, OR, XOR, NAND, NOR and INHIBT hitherto. However, the advantages of molecular logic gates include smaller size, lower power consumption and unprecedented computing performance, and thus they have potential for calculations on the nanometre scale.[15] Moreover, although great efforts have been devoted to designing either single or integrated molecular logic gates utilizing fluorescent changes with various inputs,[16] there has been no report on the use of Hg^{2+} and BSA as chemical inputs. Note Hg^{2+}-binding studies with albumin have been reported[17] to evaluate the toxicology and detoxification strategies of Hg^{2+} to humans. Also, the different combinations of these two inputs with the presence of **1** result in various outputs. This helps to program diverse logic circuits into a new type of molecular switch that can potentially be used to perform intelligent diagnostics in blood serum after exposure to Hg^{2+} sources on the nanoscale.

Results and discussion

Preparation of the compounds

The synthesis of **1** was carried out according to Scheme 1. Reaction of **L** and di-*tert*-butyl dicarbonate (Boc) forms the 3 and 9 position substituted product **2**, and the vacant 6 position was then substituted with dansyl chloride to obtain **3**, then finally the Boc group was deprotected by reacting with CF_3COOH to achieve **1**.

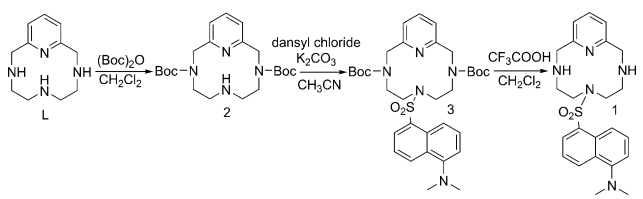

Scheme 1 Synthesis of the dansyl group appended tetraazamacrocycle sensor (**1**).

Fluorescence of 1 and its pH dependence

Firstly, the pH-dependence of the fluorescence of **1** (Fig. 1) was determined in 0.15 M NaCl aqueous solution to exclude proton disturbance in the following detection. Sensor **1** dissolves readily in water and fluoresces with λ_{em} at 550 nm at low pH. Upon increasing the pH, a blue shift of the emission spectra ($\geq\lambda$ = 23 nm) accompanied by a significant fluorescent intensity increase (inset of Fig. 1) is observed, which is analogous to the compounds reported in a previous paper.[18] The fluorescent intensity of **1** is stable at approximately pH 4.5–8.0. Therefore, all of the detections were performed in neutral Tris-HCl buffer (50 mM, pH 7.6), and the fluorescent emission band of **1** under these conditions is centred at 545 nm.

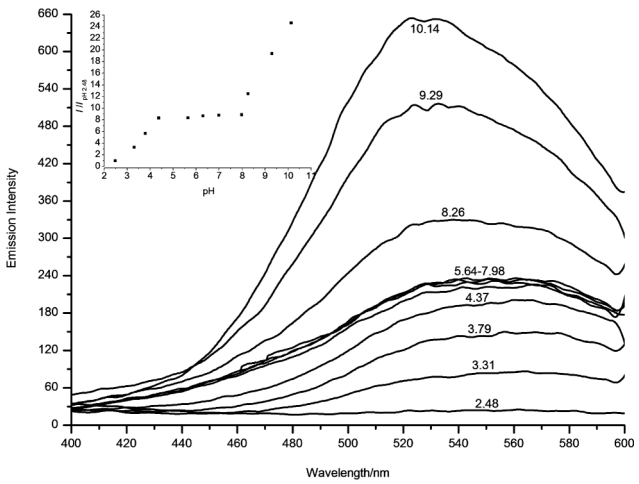

Fig. 1 Emission spectra of 10 μM **1** in water containing 0.15 M NaCl at different pH. λ_{ex} = 330 nm. Inset: The fluorescent pH titration profile of **1** according to $I/I_{pH2.48}$.

Hg^{2+} recognition by 1 in aqueous solution and its practical application

Various metal and metalloid ions (5 equiv. each) were added to Tris-HCl buffer (50 mM, pH 7.6) containing 10 μM **1**. A drastic quenching of the fluorescent emission upon the addition of Hg^{2+} is observed compared to that of only **1** in solution, and the significant blue shift from 545 to 505 nm allows for mounting ratiometric fluorescent measurements by calculating the intensity ratio at these two wavelengths (Fig. 2a). The addition of other metal ions does not induce similar results. Then, to assess the utility of **1** as a Hg^{2+}-specific fluorescent sensor, ion interference experiments were conducted in the presence of other metal cations at 5 equiv., respectively, with the subsequent addition of 1 equiv. of Hg^{2+}. As shown in Fig. 2b, the unique fluorescent response behavior of **1** towards Hg^{2+} with the ratiometric calibration (I_{505}/I_{545}) is not influenced, suggesting that Hg^{2+} could be ratiometrically recognized by **1** with high selectivity under physiological conditions.

The fluorescent response of **1** towards Hg^{2+} (Fig. 3) was further investigated in Tris-HCl buffer (50 mM, pH 7.6). The fuorescent intensity ratio (I_{505}/I_{545}) increases linearly with the concentration of Hg^{2+} (Fig. S3, ESI,† (0.1–20.0) μM, linear coefficient: R^2 = 0.9926), and further addition of Hg^{2+} does not induce any evident variation of the ratio (inset of Fig. 3). Besides, when **1** was

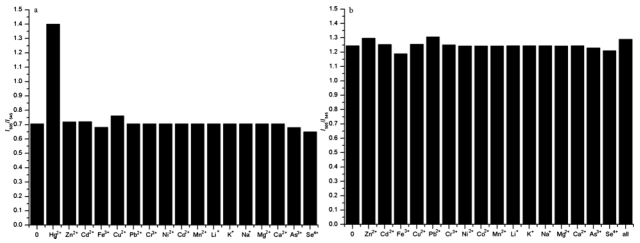

Fig. 2 (a) Ratiometric (I_{505}/I_{545}) selectivity of **1** (10 μM) upon addition of different cations (50 μM) in Tris-HCl buffer (50 mM, pH 7.6). (b) Ratiometric fluorescent response of sensor **1** (10 μM) to Hg^{2+} (10 μM) over the selected metal ions (50 μM) in Tris-HCl buffer (50 mM, pH 7.6). λ_{ex} = 330 nm.

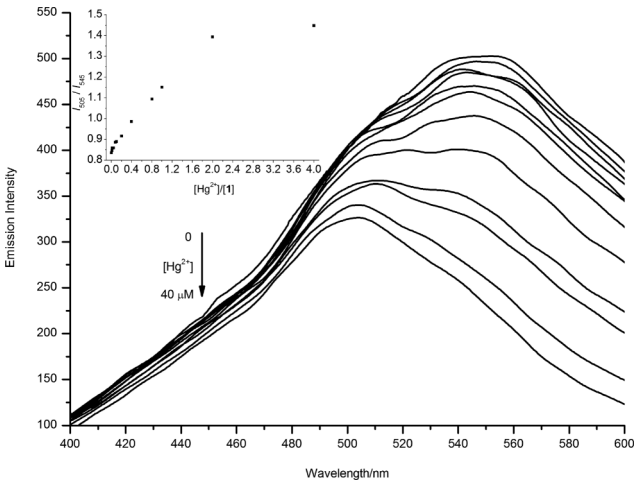

Fig. 3 Emission spectra of 10 μM **1** in Tris-HCl buffer (50 mM, pH 7.6) titrated by $HgCl_2$ solution (0–40 μM, from top to bottom). λ_{ex} = 330 nm. Inset: The fluorescent titration profile according to I_{505}/I_{545}.

employed at 5 μM, Hg^{2+} could be detected at least down to 0.5 ppb, which is lower than the U.S. Environmental Protection Agency's limit (2 ppb) for drinking water,[19] and the limit is equivalent to the Hg^{2+} concentration measured through other chemosensors.[3a,4,6,20] Furthermore, the emission ratio (I_{505}/I_{545}) of **1** is still proportional to the concentration of Hg^{2+} (Fig. S4, ESI,† (0–18) ppb, linear coefficient: $R^2 = 0.9710$). Thus, it can be concluded that the sensitivity of **1** towards Hg^{2+} is also satisfactory. Moreover, the fluorescent Job's plot indicates that **1** forms a 1 : 1 complex with Hg^{2+} (Fig. S5, ESI†), and the association constant (K_{ass}) of **1** to Hg^{2+} is determined to be about 2.6×10^6 M^{-1} by nonlinear fitting to the fluorescent titration curve[21] (Fig. S6, ESI†). In short, the decrease of the fluorescent intensity induced by Hg^{2+} is most likely attributed to the electron transfer from the excited dansyl fluorophore to the complexed Hg^{2+}.[22] In addition, the macrocycle nitrogen atom connected to the sulfonyl group is tertiary, but there is still an available electron pair to coordinate with Hg^{2+} in the ground state. The capture of Hg^{2+} by the receptor **1** decreases the electron-donating ability of the ring tertiary nitrogen to the dansyl moiety, which inhibits the internal charge transfer (ICT) between them and thus results in the hypsochromic shift of the emission band.[23]

It is worth noting that the S–N bond of the dansyl-macrocycle has been reported to be photochemically cleaved in the presence of metal ions.[24] Thus, the effect of Hg^{2+} (5 equiv.) on the photolysis of **1** in Tris-HCl buffer (50 mM, pH 7.6) was tested. The change in emission intensity at 505 nm of **1** after UV irradiation at 330 nm for 40 min compared to that before UV irradiation in the presence of Hg^{2+} is negligible (Fig. S7, ESI†), demonstrating that the photolysis of **1** does not take place in this process.

The Hg^{2+} binding behavior of **1** was further investigated by UV-vis titrations. The UV spectra (Fig. S8, ESI†) exhibit two superimposed bands with contribution from two chromophores (pyridine and dansyl). The pyridine absorption of free **1** at about 250 nm gradually increases, whereas the typical dansyl absorption at 329 nm increases and undergoes a red shift of 7 nm as 1 equiv. of Hg^{2+} was added, and thereafter it remains almost unchanged. The enhancement and bathochromic shift of the spectra indicate the interaction of Hg^{2+} with **1**. Meanwhile, the absence of the band at 286 nm, which originates from the protonation of dimethylamino group of the dansyl fragment,[12a,25] indicates that Hg^{2+} probably interacts with the sulfonyl group rather than the dimethylamino group of dansyl.

Moreover, theoretical calculations were executed to clarify the coordination geometry of **1** and **1**-Hg^{2+}. The optimized structure of **1**-Hg^{2+} indicates that a stable complex with significant conformation changes is formed compared to that of **1** (Fig. 4). The lone pair electrons on N2 and N4 are orientated towards bound Hg^{2+}, and one oxygen atom of the sulfonyl group (O1) also rotates and increases in proximity to Hg^{2+}. The calculated mercury–nitrogen bond distances (Hg–N1 = 2.26 Å, Hg–N2 = 2.47 Å, Hg–N3 = 2.41 Å, Hg–N4 = 2.45 Å) are shorter than the upper limit of 2.75 Å for the typical covalent bond distance of Hg and N.[26] Besides, O1 is 2.26 Å distant from Hg^{2+}, which is smaller than the sum of the van der Waals radii of Hg and O (2.9 Å).[27] Thus, it can be concluded that Hg^{2+} is stabilized by coordination with the macrocycle nitrogen atoms and sulfonyl of the dansyl group, which is in accordance with the fluorescence and UV changes of **1** after binding to Hg^{2+} discussed above.

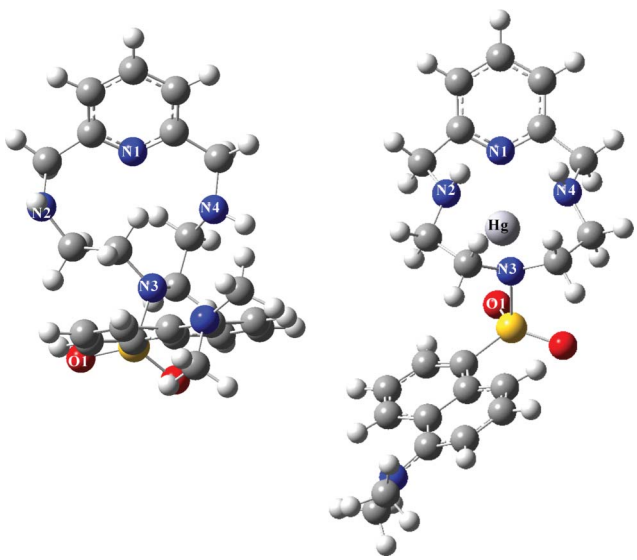

Fig. 4 Optimized geometries of **1** and **1**-Hg^{2+} calculated by DFT methods.

Furthermore, reversibility, which is essential for attributing a signal to Hg^{2+} and for recycling of the indicator, is thus universally recognized as one of the most desirable properties of a qualified chemosensor.[3a,28] To examine the reversibility of **1**-Hg^{2+}, EDTA

was exploited as an external additive for its extremely high formation constant with Hg^{2+} ($K_f = 6.3 \times 10^{21}$ at 20 °C).[29] The blue shift and fluorescent quenching of **1** induced by Hg^{2+} are completely recovered upon addition of 1 equiv. of EDTA (Fig. S9, ESI†). Thus, **1** was verified to be a reversible chemosensor for Hg^{2+}.

As a bonus of the above results, the emission color of **1** changes from orange to green (Fig. 5a) upon the addition of Hg^{2+} (1 equiv.), which can be detected by the naked eye. Consequently, test strips absorbing sensor **1** were prepared and dipped into Hg^{2+} aqueous solutions of different concentration to investigate its practical value. Apparent color changes excited by a UV lamp at 365 nm can be observed (Fig. 5b) and the discernible concentration of Hg^{2+} is approximately above 10^{-7} M. Thus, this method has been validated to be convenient and sensitive for the fast detection of Hg^{2+}.

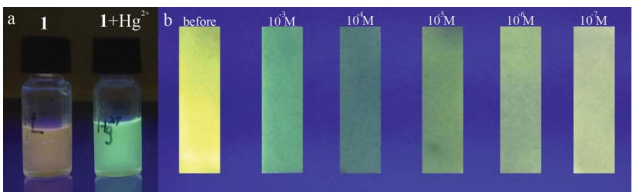

Fig. 5 Photographs of (a) fluorescent color changes of 10 μM **1** upon the addition of Hg^{2+} (1 equiv.) in Tris-HCl buffer (50 mM, pH 7.6) and (b) its application for the test paper with different Hg^{2+} concentrations under the UV lamp (λ_{ex} = 365 nm).

In vitro studies have demonstrated the ability of **1** to detect Hg^{2+} with excellent selectivity. To further confirm the applicability of **1** *in vivo*, inverted fluorescence microscopy images were investigated to detect exogenous mercury ions with **1** in living cells. Bright field image measurements confirm that the cells are viable throughout the imaging studies (Fig. 6a). After treatment of HeLa cells with **1** (50 μM) alone for 15 min at 37 °C, the cells exhibit strong yellow-green fluorescence upon excitation with UV light (Fig. 6b). Upon addition of Hg^{2+} (50 μM) and incubation for another 30 min at 37 °C, the cells show a relatively weak green fluorescence signal (Fig. 6c), indicating

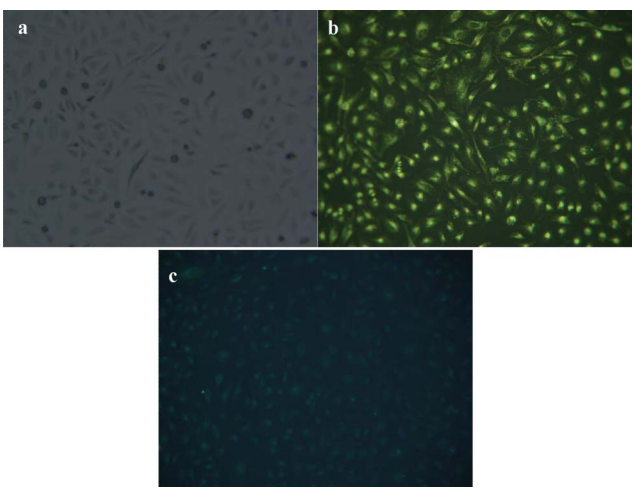

Fig. 6 (a) Bright field image of HeLa cells incubated with **1** (50 μM) for 15 min. (b) Fluorescence image of HeLa cells incubated with **1** (50 μM) for 15 min. (c) Fluorescence image of HeLa cells incubated with **1** (50 μM) for 15 min, washed three times, and then further incubated with 50 μM Hg^{2+} for 30 min.

that the fluorescence of **1** is slightly quenched and blue-shifted by the response of **1** to Hg^{2+} ions. The cell experiment is not only in accordance with the investigation of **1** in solution, but also shows that **1** is easily cell-permeable and can be used to monitor the process of visible fluorescence (from yellow-green to green) responses to Hg^{2+} in living cells.

BSA recognition by 1 in aqueous solution and its practical application

Taking into consideration that the fluorescence of **1** is expected to change between bulk solution and a non-polar environment owing to the solvatochromic dansyl group, the fluorescent response of **1** upon adding a few selected proteins (2 μM) was tested in Tris-HCl buffer (50 mM, pH 7.6). As shown in Fig. 7, trypsin and lysozyme merely induce negligible fluorescent variations, and the addition of egg albumin slightly enhances the emission intensity at 545 nm. In particular, only with BSA does a structured band with an emission maximum at 445 nm appear. It has been reported that hydrophobic pockets in serum albumin tend to bind organic compounds containing aromatic cycles.[30] As the donor site dimethylamino of the dansyl group is connected by a single bond to the naphthalene ring, a twisted intramolecular charge transfer (TICT) phenomenon would consequently occur.[31] Therefore, the emission band at longer wavelength can be ascribed to the TICT state, in which the donor and acceptor naphthalene sulfonyl are orthogonal to each other.[28a] Besides, fluorescent emission of **1** in the presence of a less polar solvent (MeCN) without BSA was examined, and the emission band centered at 445 nm can also be observed (Fig. S10, ESI†). Thus, the newly emerged emission band at 445 nm can be attributed to the locally excited (LE) state, which arises from the intramolecular charge transfer from the donor to the acceptor with a corresponding twist of the donor residue about the bond (Scheme 2).

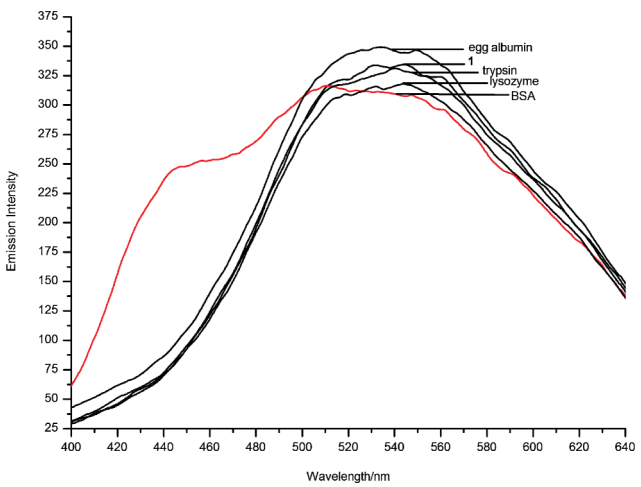

Fig. 7 Emission spectra of 10 μM **1** in the presence of various proteins (2 μM) in Tris-HCl buffer (50 mM, pH 7.6). λ_{ex} = 330 nm.

Fig. 8 explains the dependence of the fluorescent spectra of **1** in Tris-HCl (50 mM, pH 7.6) on the BSA concentration. The TICT band of **1** centered at 545 nm apparently shifts to 505 nm with an intense enhancement in the fluorescent intensity of both LE and TICT bands upon adding BSA. An increase of BSA concentration

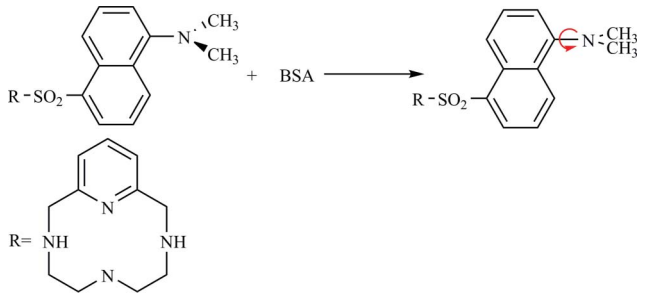

Scheme 2 Origin of the LE state of **1** *via* interaction with BSA.

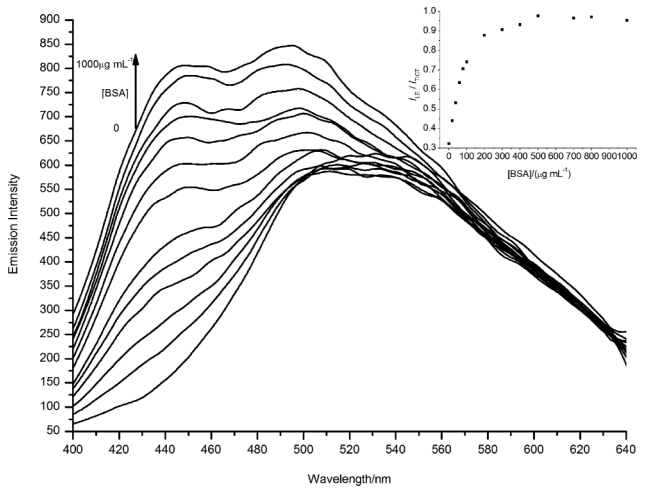

Fig. 8 Emission spectra of 10 μM **1** upon the addition of BSA (0–1000 μg mL^{-1}) in Tris-HCl buffer (50 mM, pH 7.6). Inset: Dependence of I_{LE}/I_{TICT} on the concentration of BSA. λ_{ex} = 330 nm.

leads to lower polarity, which destabilizes the excited state more than the ground state. The energy gap between the emitting and the ground state consequently increases, which results in the blue-shift of the TICT band. A similar fluorescent change of the TICT band also occurs in MeCN solution containing **1** compared to that in the aqueous solution (Fig. S10, ESI†). As shown in the inset of Fig. 8, the emission intensity ratio (I_{LE}/I_{TICT}) indicates that the LE state is more sensitive than the TICT state at low BSA concentration, and the ratio gradually levels off above 400 μg mL^{-1} BSA. This phenomenon signifies that the formation of the TICT state is reduced by the non-polar environment in the hydrophobic cavity of BSA, which leads to the equilibrium shift from the TICT state to the LE state.[32] Moreover, the linear range for detecting BSA utilizing I_{LE}/I_{TICT} as the calibration is 0–100 μg mL^{-1} with the limit of 1 μg mL^{-1} (Fig. S11, ESI,† linear coefficient: R^2 = 0.9917), which makes **1** applicable for the determination of unknown concentrations of albumin in serum samples.

The binding pattern of sensor **1** with BSA was further investigated. Urea-induced unfolding of BSA was studied to clarify whether the interaction of **1** and BSA is a noncovalent one.[33] As shown in Fig. S12, ESI,† the emission intensity ratio (I_{LE}/I_{TICT}) of **1** after the addition of 1 equiv. of BSA is decreased in a stepwise manner by the addition of urea, suggesting that BSA binds to **1** in its native form and denaturation of BSA by the urea results in the release of **1** from the non-polar environment to the bulk aqueous solution. Therefore, sensor **1** has been demonstrated to function as a noncovalent-labeling bioprobe in BSA detection. Besides, the fluorescent intensity at 445 nm is nonlinearly fitted into the Hill equation[34] as follows (Fig. S13, ESI†):

$$\log(I_{445} - I_{min})/(I_{max} - I_{445}) = n\log[\text{BSA}] + \log K \quad (1)$$

The binding constant (log$K$) of **1** to BSA is determined to be 7.4, and the Hill coefficient is estimated to be 1.3, which indicates a positive cooperativity. This coefficient can be interpreted such that the minimum number of BSA interacting binding sites for **1** is one. Moreover, the fluorescent Job's plot carried out between **1** and BSA is conducted to determine the maximum binding site number of **1**-BSA, and the result unequivocally determines that the binding stoichiometry is 1 : 4 (Fig. S14, ESI†), suggesting four noncovalent binding sites for each protein.

Apart from investigating the interaction of **1** and BSA in solution, **1** was applied to stain various concentrations of BSA after electrophoresis using 1-D SDS-PAGE gels, which were scanned using the image analysis systems before and after washing **1** away. In other words, nonprotein substances such as inorganic salts, detergents and chelating reagents did not interfere with albumin quantification in the gel. Fig. 9a and 9b show that the gel images of BSA samples after staining, which demonstrate the stable binding of **1** with BSA and that a visual fluorescent examination of the staining response is successful. Commonly utilized fluorescent dyes such as SYPRO Ruby[35] cannot stain proteins in the presence of SDS, and it takes a long time for staining (overnight) and washing the gels to completely eliminate SDS and excess dyes (60 min). In contrast, the staining procedure of compound **1** with the detection limit of 0.4 μg/well required only 60 min, and fluorescent images of BSA could be obtained whether SDS and excess dyes in the gel have been removed (30 min) or not. Besides, the integrated volume of the densitometry units of the scanned bands of the proteins in the gel is observed to increase linearly with increasing BSA concentration on staining with **1** (Fig. 9c, linear coefficient: R^2 = 0.9913), indicating that **1** is also an appropriate candidate for rapid albumin staining and quantitative detection.

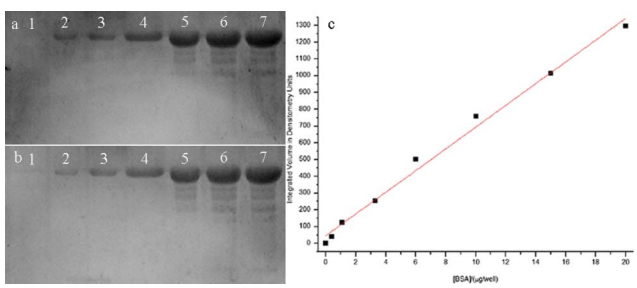

Fig. 9 Staining protocol for BSA using **1** after SDS-PAGE (a) Typical gel images of BSA before washing; (b) after washing. The amount of BSA in each well is as follows: (1) 0.4 μg; (2) 1.1 μg; (3) 3.3 μg; (4) 6.0 μg; (5) 10.0 μg; (6) 15.0 μg; (7) 20.0 μg. (c) The relation between the integrated volume in densitometry units for scanned bands and the BSA concentrations.

As mentioned above, it is feasible to apply the linear increasing range of the fluorescent emission intensity ratio (I_{LE}/I_{TICT}) as the calibration curve to determine BSA concentration in fetal bovine serum. The serum contains numerous salts, glucose, hormones and proteins other than albumin,[36] which may bring potential interference to the fluorescence of **1**. Nevertheless, the results are still unaffected and in good agreement with those using UV

Table 1 Analytical application of the proposed method

Method	BSA added (mg mL^{-1})	Found (mg mL^{-1}) Mean[a] ± SD[b]	Recovery (%)
Proposed method	0	38.10	—
	0.02	38.13 ± 0.01	100.03
UV detection	0	39.06	—
	0.30	39.41 ± 0.04	100.89

[a] Mean of the three determinations. [b] SD: standard deviation.

detection (Table 1), which is commonly exploited for analyzing the album concentration in blood serum.[37] Thus, the proposed method has been justified to be valid and effective. Besides, although other chemosensors have been reported for application to the fluorescent determination of BSA concentrations in serum,[9] **1** is used for the first time to set up a ratiometric fluorescent assay, which will be of pronounced significance in biological systems by providing a built-in correction for environmental effects.

Logic behavior of 1 with Hg^{2+} and BSA as inputs

Apart from the above attempted analytical applications, **1** was also implemented to follow logic gate operations using Hg^{2+} and BSA as chemical inputs. The original fluorescent peak of **1** at 545 nm, the new emission band centered at 445 nm, and the band formed (505 nm) owing to the blue-shift of the original one are all defined as 'True' outputs, or binary '1'. On the contrary, disappearance of any of the fluorescent emission bands centered at the three wavelengths then corresponds to a 'False' output, or binary '0'. Adding 1 equiv. of Hg^{2+} to the Tris-HCl (50 mM, pH 7.6) buffer containing 10 μM **1** quenches its fluorescent intensity at 545 nm and the spectrum hypsochromically shifts to 505 nm (Fig. 10a). The addition of 200 μg mL^{-1} BSA enhances the fluorescence of **1** at 445 nm as well as causing the fluorescent band centered at 545 nm to shift to 505 nm. Besides, simultaneous existence of Hg^{2+} and BSA quenches the fluorescent intensity of **1** at both 445 nm and 505 nm compared to the solution merely containing **1** and BSA, but the shape of its fluorescent spectrum does not vary noticeably. Accordingly, a truth table (Table 2) and logic circuit (Fig. 10b) composed of three different logic gates are constructed from the above fluorescent behaviors of **1**, representing YES, OR, and NOR logic gates, respectively. The function of OR effectively finds the maximum between two binary digits, and the NOR gate is highly significant in electronics for its ability to be combined to form any other type of logic gate. Moreover, the combination of the intrinsic properties with selective actions by different

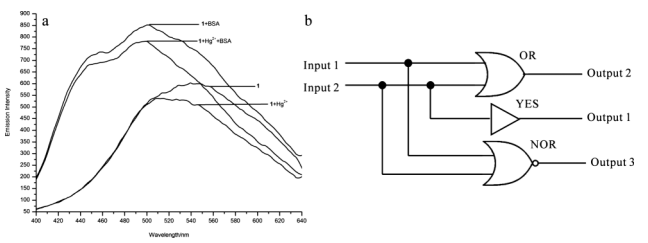

Fig. 10 (a) Fluorescent spectra of 10 μM **1**, 10 μM **1** and Hg^{2+}, 10 μM **1** and 200 μg mL^{-1} BSA, and their coexistence in Tris-HCl buffer (50 mM, pH 7.6). λ_{ex} = 330 nm. (b) Combinatorial logic circuit of a triple output molecular switch.

Table 2 Truth table

	Input 1	Input 2	Output 1	Output 2	Output 3
Entry	Hg^{2+}	BSA	445 nm	505 nm	545 nm
1	0	0	0	0	1
2	1	0	0	1	0
3	0	1	1	1	0
4	1	1	1	1	0

chemical inputs allows the application of **1** to design a complicated molecular switch to smartly diagnose the toxicity of Hg^{2+} in the close proximity of albumin on the nanoscale, which is expressed in terms of a simple computer program (using C language, see the ESI†), aiming to mimic the operation of semiconductor logic gates.

Conclusions

In summary, we have designed and synthesized a novel fluorescent probe **1** for the ratiometric recognition of Hg^{2+} and BSA with different modes in aqueous solution at physiological pH. The water soluble sensor **1** employing a dansyl fluorophore exhibits selective quenching and a blue shift response to at least 0.5 ppb Hg^{2+}, and responds to concentrations above 1 μg mL^{-1} BSA selectively *via* noncovalent interactions. Sensor **1** has been successfully applied to a fast Hg^{2+} test paper assay, and **1** has also been verified to be easily cell-penetrable and applicable for Hg^{2+} fluorescent imaging in living HeLa cells. Imaging of BSA in the gel using SDS-PAGE stained in the medium containing **1** demonstrated that the binding of **1** and BSA was feasible in the presence of nonprotein substances. Besides, the versatile performance of **1** has also been applied to albumin concentration determination in blood serum exploiting the ratiometric fluorescent calibration curve. Finally, the multiple input/output characteristics of **1** toward Hg^{2+} and BSA have been utilized to construct a complex molecular switch consisting of three logic gates, which will be promising in intelligent diagnostics for Hg^{2+} contaminated serum on the nanometre scale.

Experimental

General

All the starting materials were of reagent quality and were obtained from commercial sources without further purification. Lysozyme (egg white) was bought from Amresco, trypsin and egg albumin were purchased from Nanjing Zhuyan Biotechnology Co., Ltd. Dulbecco's Modified Eagle's Medium (DMEM) was bought from Gibco. Fetal bovine serum (FBS) was bought from Hangzhou Sijiqing Biological Engineering Materials Co., Ltd. ^{1}H NMR spectra were determined using a Bruker

DRX-500 spectrometer at 25 ± 1 °C. All the UV-vis spectra were recorded by a Shimadzu UV-3100 spectrophotometer. The emission spectra were obtained using a PerkinElmer LS 55 fluorescence spectrometer. The pH values of sample solutions were monitored by a PHS-3 system. The electrospray ionization mass spectra were determined by a LCQ Fleet ThermoFisher mass spectrometer. 1,4,7-Tritosyl-1,4,7-triazaheptane was prepared according to a reported procedure[38] in 62% yield after crystallization. 2,6-Bis(bromomethyl)pyridine and the mother ring 3,6,9,15-tetraazabicyclo[9.3.1] pentadeca-1(15),11,13-triene (L) were synthesized following the procedure described by the references[39] in yields of 49% and 65%, respectively.

Preparation of the compounds

3,6,9,15-Tetraazabicyclo[9.3.1]pentadeca-1(15),11,13-triene-3,9-dicarboxylic acid bis-*tert*-butylester (2). A solution of di-*tert*-butyl dicarbonate (2.02 g, 9.25 mmol) in CH_2Cl_2 (35 mL) was added dropwise to a stirred solution of **L** (1.03 g, 5 mmol) in CH_2Cl_2 (130 mL). The mixture was stirred at room temperature for 18 h. The solvent was then removed under reduced pressure to yield a yellow oil, which was purified by column chromatography on silica with CH_2Cl_2/EtOH/NH_3·H_2O (10 : 1 : 0.1 v:v:v; R_f 0.32) and a yellow oil was obtained (1.12 g, 55%). ^{1}H NMR (500 MHz, $CDCl_3$): δ_H 7.87 (t, J = 8 Hz, 1H), 7.24 (d, J = 8 Hz, 2H), 4.77 (br s, 9H), 3.58 (s, 4H), 1.63 (s, 18H); Mass: ES-MS (CH_3CN), m/z (%): 407.42 $[M+H]^+$.

6-(1-(Dimethylamino)-5-naphthalene sulfonyl)-3,6,9,15-tetraazabicyclo[9.3.1]pentadeca-1(15),11,13-triene-3,9-dicarboxylic acid bis-*tert*-butylester (3). A mixture of dansyl chloride (0.048 g, 0.18 mmol), **2** (0.072 g, 0.18 mmol) and 0.49 g K_2CO_3 in 9 mL of CH_3CN was stirred under a nitrogen atmosphere at room temperature for 4 days. After filtration of the K_2CO_3, the solvent was evaporated and **3** was isolated as a green powder (0.056 g, 49%) by column chromatography on silica with CH_2Cl_2/EtOH (30 : 1 v:v; R_f 0.44). Mass: ES-MS (CH_3CN), m/z (%): 640.50 $[M+H]^+$, 662.42 $[M+Na]^+$.

6-(1-(Dimethylamino)-5-naphthalene sulfonyl) -3,6,9,15-tetraazabicyclo [9.3.1] pentadeca- 1(15),11,13-triene (1). Compound **3** (0.076 g, 0.12 mmol) was stirred in 2.8 mL of CF_3COOH/CH_2Cl_2 (1 : 1) under a nitrogen atmosphere at room temperature for 3 h. The pH of the solution was then adjusted to 12 using 2 M NaOH and the aqueous layer was extracted with CH_2Cl_2. The organic layer was dried over Na_2SO_4 and the solvent was evaporated to yield a yellow-green powder (0.041 g, 78%). ^{1}H NMR (500 MHz, $CDCl_3$): δ_H 8.55 (d, J = 8.5 Hz, 1H), 8.47 (d, J = 8.5 Hz, 1H) 8.22 (d, J = 6.5 Hz, 1H), 7.62 (t, J = 7.2 Hz, 1H), 7.54 (m, 2H), 7.19 (d, J = 7 Hz, 1H), 7.06 (d, J = 7.5 Hz, 2H), 4.22 (s, 4H), 3.59 (br s, 6H), 2.89 (s, 6H), 2.86 (s, 4H) ppm; Mass: ES-MS (CH_3CN), m/z (%): 440.33 $[M+H]^+$.

Spectroscopic study

The emission spectra of **1** (10 μM) were determined in Tris-HCl buffer (50 mM, pH 7.6). The pH dependence of emission was determined in 0.15 M NaCl aqueous solution at different pH values adjusted by 1 M HCl and 1 M NaOH. The excitation wavelength was 330 nm.

Selective fluorescent response of 1 to different metal cations

The fluorescent response of **1** to different metal cations was examined in Tris-HCl buffer (50 mM, pH 7.6) containing 10 μM **1**. Metal cation aqueous solutions (10 μL, 10 mM) were added to 2 mL of this solution, and the fluorescent spectra were determined after complete mixing.

Hg^{2+} titration of a solution of 1 determined by fluorescence and UV

The fluorescent titration of **1** was investigated by adding aliquots of 0.4 μL of $HgCl_2$ aqueous solution (1 mM) to 2 mL of a solution of **1** (10 μM, 50 mM Tris-HCl, pH 7.6) in a cuvette. The spectra were recorded immediately after mixing. The UV titration experiments were performed in a similar manner. Aliquots of 5 μL of $HgCl_2$ solution (1 mM) were added to 1 mL of a solution of **1** (50 μM, 50 mM Tris-HCl, pH 7.6).

Computational details

The ground state structures of **1** and **1**-Hg^{2+} were computed utilizing the density functional theory (DFT) method with the hybrid density functional Becke-3-Lee–Yang–Parr (B3LYP). Double valence 3-21 g basis set was used for nonmetal elements (C, H, N, S, and O), which reasonably balances the computational cost and the reliability of the results.[40] An effective core potential LanL2DZ basis set was defined for Hg to incorporate the relativistic corrections. All of the theoretical calculations were carried out using the Gaussian98 program package.[41]

EDTA titration of 1-Hg^{2+} determined by fluorescence

The reversibility of **1** towards Hg^{2+} was conducted by first adding 2 μL of Hg^{2+} (10 mM) to 2 mL Tris-HCl buffer (50 mM, pH 7.6) containing 10 μM **1**. Then 2 μL of EDTA (10 mM) was added into the above solution. Fluorescence spectra were all recorded after complete mixing.

Test paper assay for the detection of Hg^{2+} by 1

Test strips were prepared by immersing the filter paper into Tris-HCl buffer (50 mM, pH 7.6) containing **1** (100 μM) and then drying in air. Then the test papers achieved were dipped into Hg^{2+} aqueous solutions of different concentration (10^{-7} M–10^{-3} M), and were excited by the UV lamp (365 nm) to observe the color changes.

Cell culture methods

HeLa cells were grown in DMEM medium supplemented with 10% freshly inactivated FBS and were seeded equivalently into 96-well plates. The plates were kept at 37 °C in a humidified atmosphere of 5% CO_2 and allowed to adhere for 24 h.

Fluorescence imaging

After the HeLa cells had been washed with phosphate-buffered saline (PBS, 50 mM, pH 7.4), 50 μM **1** in PBS was added to the cells. The cells were then incubated for 15 min at 37 °C. Cell imaging was carried out after washing of the cells with PBS utilizing inverted fluorescence microscopy (OLYMPUS DP72, Japan, with a UV filter). The cells were further treated with $HgCl_2$ solution

(50 μM) in PBS for another 30 min at 37 °C. The treated cells were immediately imaged in the same way.

Selective fluorescent response of 1 to different proteins

The fluorescent response of **1** to different proteins was investigated using 2 mL of a solution of **1** (10 μM, 50 mM Tris-HCl, pH 7.6) in a cuvette. The experiment was carried out by adding 2.7 μL of protein aqueous solution (1.5 mM) to the obtained solution. The spectra were recorded immediately after mixing.

BSA titration of a solution of 1 determined by fluorescence

The fluorescent titration was carried out in 2 mL Tris-HCl buffer (50 mM, pH 7.6) containing 10 μM **1**. Then the fluorescent titration was investigated by adding aliquots of 1.3 μL of BSA aqueous solution (150 μM) to the obtained solution. All of the spectra were recorded after complete mixing.

Urea titration of 1-BSA determined by fluorescence

First, 13.3 μL of BSA (1.5 mM) was added to 2 mL Tris-HCl buffer (50 mM, pH 7.6) containing 10 μM **1**. The fluorescent titration was then investigated by adding aliquots of 130 μL of urea aqueous solution (15.1 M) to the obtained **1**-BSA solution. The fluorescence spectra were all determined after complete mixing.

SDS-PAGE measurements

The determination of BSA separated by SDS-PAGE and stained with **1** was carried out using a Bio-Rad Mini-PROTEAN Tetra System. Compound **1** was dissolved in a mixture of AcOH, MeOH, and H_2O (AcOH/MeOH/H_2O = 3 : 10 : 87, v:v:v) with a concentration of 10 μM. After SDS-PAGE, the gel was stained using the above solution containing **1** for 60 min, and then washed with the solution (AcOH/MeOH/H_2O = 3 : 10 : 87, v:v:v) for 30 min. The image acquisition and analysis were carried out using Bio-Rad imaging system before and after washing the gels.

BSA concentration determination in blood serum by 1 utilizing fluorescence and UV

In the proposed fluorescent detection, fetal bovine serum (2.5 μL) was added to 2 mL Tris-HCl buffer (50 mM, pH 7.6) containing 10 μM **1**, *i.e.*, blood serum was diluted by 800 times to lie in the calibration curve of **1** towards BSA. The fluorescent spectrum was then recorded after complete mixing. In the UV experiment, serum (100 μL) was added to 1 mL Tris-HCl buffer (50 mM, pH 7.6) containing 10 μM **1**, then the protein in solution was determined by examining the absorption at 280 nm. Each of the two methods was measured three times to ensure accuracy.

Acknowledgements

This work is supported by the National Natural Science Foundation of China (21021062, 21027013, 21075064 and 90813020) and the National Basic Research Program of China (2007CB925102).

Notes and references

1 (*a*) T. Takeuchi, N. Morikawa, H. Matsumoto and Y. Shiraishi, *Acta Neuropathol.*, 1962, **2**, 40–57; (*b*) M. Harada, *Crit. Rev. Toxicol.*, 1995, **25**, 1–24; (*c*) P. Grandjean, P. Weihe, R. F. White and F. Debes, *Environ. Res.*, 1998, **77**, 165–172.
2 H. A. Mckenzie and L. E. Smythe, *Quantitative trace analysis of biological materials.* New York: Elsevier, 1998.
3 (*a*) E. M. Nolan and S. J. Lippard, *Chem. Rev.*, 2008, **108**, 3443–3480 and the references within; (*b*) D. W. Domaille, E. L. Que and C. J. Chang, *Nat. Chem. Biol.*, 2008, **4**, 168–175.
4 A few selected examples: (*a*) R. H. Yang, W. H. Chan, A. W. Lee, P. F. Xia, H. K. Zhang and K. Li, *J. Am. Chem. Soc.*, 2003, **125**, 2884–2885; (*b*) T. J. Dickerson, N. N. Reed, J. J. LaClair and K. D. Janda, *J. Am. Chem. Soc.*, 2004, **126**, 16582–16586; (*c*) A. Caballero, R. Martinez, V. Lloveras, I. Ratera, J. Vidal-Gancedo, K. Wurst, A. Tarraga, P. Molina and J. Veiana, *J. Am. Chem. Soc.*, 2005, **127**, 15666–15667; (*d*) J. Wang and X. Qian, *Chem. Commun.*, 2006, 109–111; (*e*) Y. Zhao and Z. Zhong, *J. Am. Chem. Soc.*, 2006, **128**, 9988–9989; (*f*) M.-L. Ho, K.-Y. Chen, L.-C. Wu, J.-Y. Shen, G.-H. Lee, M.-J. Ko, C.-C. Wang, J.-F. Lee and P.-T. Chou, *Chem. Commun.*, 2008, 2438–2440; (*g*) C.-W. Liu, C.-C. Huang and H.-T. Chang, *Anal. Chem.*, 2009, **81**, 2383–2387; (*h*) M. Kumar, A. Dhir and V. Bhalla, *Chem. Commun.*, 2010, **46**, 6744–6746; (*i*) Z. Guo, W. Zhu, M. Zhu, X. Wu and H. Tian, *Chem.–Eur. J.*, 2010, **16**, 14424–14432; (*j*) S. Ando and K. Koide, *J. Am. Chem. Soc.*, 2011, **133**, 2556–2566; (*k*) H. Yu, Y. Xiao, H. Guo and X. Qian, *Chem.–Eur. J.*, 2011, **17**, 3179–3191; (*l*) A. Mitra, A. K. Mittal and C. P. Rao, *Chem. Commun.*, 2011, **47**, 2565–2567.
5 (*a*) G. Grynkiewicz, M. Poenie and R. Y. Tsien, *J. Biol. Chem.*, 1985, **260**, 3440–3450; (*b*) S. Deo and H. A. Godwin, *J. Am. Chem. Soc.*, 2000, **122**, 174–175; (*c*) J. V. Mello and N. S. Finney, *Angew. Chem., Int. Ed.*, 2001, **40**, 1536–1538; (*d*) M. S. Tremblay, M. Halim and D. Sames, *J. Am. Chem. Soc.*, 2007, **129**, 7570–7577; (*e*) Z. Xu, N. J. Singh, J. Lim, J. Pan, H. N. Kim, S. Park, K. S. Kim and J. Yoon, *J. Am. Chem. Soc.*, 2009, **131**, 15528–15533.
6 (*a*) E. M. Nolan and S. J. Lippard, *J. Mater. Chem.*, 2005, **15**, 2778–2783 ; (*b*) J. Wang, X. Qian and J. Cui, *J. Org. Chem.*, 2006, **71**, 4308–4311; (*c*) E. M. Nolan and S. J. Lippard, *J. Am. Chem. Soc.*, 2007, **129**, 5910–5918; (*d*) M. Tian and H. Ihmels, *Chem. Commun.*, 2009, 3175–3177.
7 G. Zolese, G. Falcioni, E. Bertoli, R. Galeazzi, M. Wozniak, Z. Wypych, E. Gratton and A. Ambrosini, *Proteins: Struct., Funct., Genet.*, 2000, **40**, 39–48.
8 P. D. Berk and K. M. Korenblat, In *Approach to the patient with jaundice or abnormal liver test results*, 23rd ed.; L. Goldman and D. Ausiello, ed.; Saunders Elsevier: Philadelphia, 2007; chap 150.
9 (*a*) R. Haughland, *Handbook of Fluorescent Probes and Research Chemicals Molecular Probes*M. Inc.: Eugene, OR, 1996; (*b*) D. H. Li, H. H. Yang, H. Zhen, Y. Fang, Q. Z. Zhu and J. G. Xu, *Anal. Chim. Acta*, 1999, **401**, 185–189; (*c*) C. Jiang and L. Luo, *Anal. Chim. Acta*, 2004, **506**, 171–175; (*d*) Z. Xu, W. Yang and C. Dong, *Bioorg. Med. Chem. Lett.*, 2005, **15**, 4091–4096; (*e*) X. Chen, Y. Xiang and A. Tong, *Talanta*, 2010, **80**, 1952–1958.
10 Y. Shiraishi, S. Sumiya, Y. Kohno and T. Hirai, *J. Org. Chem.*, 2008, **73**, 8571–8574.
11 (*a*) S.-Y. Moon, N. J. Youn, S. M. Park and S.-K. Chang, *J. Org. Chem.*, 2005, **70**, 2394–2397; (*b*) S. H. Kim, J. S. Kim, S. M. Park and S.-K. Chang, *Org. Lett.*, 2006, **8**, 371–374; (*c*) S. M. Park, M. H. Kim, J.-I. Choe, K. T. No and S.-K. Chang, *J. Org. Chem.*, 2007, **72**, 3550–3553; (*d*) P. Mahato, A. Ghosh, S. Saha, S. Mishra, S. K. Mishra and A. Das, *Inorg. Chem.*, 2010, **49**, 11485–11492.
12 (*a*) R. Métivier, I. Leray and B. Valeur, *Photochem. Photobiol. Sci.*, 2004, **3**, 374–380; (*b*) J. Guy, K. Caron, S. Dufresne, S. W. Michnick, W. G. Skene and J. W. Keillor, *J. Am. Chem. Soc.*, 2007, **129**, 11969–11977; (*c*) M. H. Lee, H. J. Kim, S. Yoon, N. Park and J. S. Kim, *Org. Lett.*, 2008, **10**, 213–216.
13 (*a*) K. P. Ghiggino, A. G. Lee, S. R. Meech, D. V. O'Connor and D. Phillips, *Biochemistry*, 1981, **20**, 5381–5389; (*b*) C. M. Cardona, J. Alvarez, A. E. Kaifer, T. D. McCarley, S. Pandey, G. A. Baker, N. J. Bonzagni and F. V. Bright, *J. Am. Chem. Soc.*, 2000, **122**, 6139–6144; (*c*) O. Hayashida and I. Hamachi, *J. Org. Chem.*, 2004, **69**, 3509–3516; (*d*) P. M. Page, T. A. McCarty, G. A. Baker, S. N. Baker and F. V. Bright, *Langmuir*, 2007, **23**, 843–849.
14 (*a*) A. S. Bhown, T. W. Cornelius, J. E. Volanakis and J. C. Bennett, *Anal. Biochem.*, 1983, **131**, 337–340; (*b*) D. L. Sackett and J. Wolff, *Anal. Biochem.*, 1987, **167**, 228–234; (*c*) J. R. Daban, M. Samso and S. Bartolome, *Anal. Biochem.*, 1991, **199**, 162–168; (*d*) J. R. Daban, S. Bartolome and M. Samso, *Anal. Biochem.*, 1991, **199**, 169–174; (*e*) Y. Suzuki and K. Yokoyama, *J. Am. Chem. Soc.*, 2005, **127**, 17799–17802; (*f*) V. S. Jisha, K. T. Arun, M. Hariharan and D. Ramaiah, *J. Am.*

Chem. Soc., 2006, **128**, 6024–6025; (*g*) C. A. Royer, *Chem. Rev.*, 2006, **106**, 1769–1784; (*h*) B. K. Paul, A. Samanta and N. Guchhait, *J. Phys. Chem. B*, 2010, **114**, 6183–6196; (*i*) J.-S. Lee, H. K. Kim, S. Feng, M. Vendrell and Y.-T. Chang, *Chem. Commun.*, 2011, **47**, 2339–2341; (*j*) K. Kudo, A. Momotake, Y. Kanna, Y. Nishimura and T. Arai, *Chem. Commun.*, 2011, **47**, 3867–3869.

15 S. E. Thompson and S. Parthasarathy, *Mater. Today*, 2006, **9**, 20–25.

16 (*a*) A. P. de Silva, H. Q. N. Gunaratne and C. P. McCoy, *Nature*, 1993, **364**, 42–44; (*b*) A. W. Czarnik, *Acc. Chem. Res.*, 1994, **27**, 302–308; (*c*) A. P. de Silva, H. Q. N. Gunaratne, T. A. Gunnlaugsson, T. M. Huxley, C. P. McCoy, J. T. Rademacher and T. E. Rice, *Chem. Rev.*, 1997, **97**, 1515–1566; (*d*) T. H. Lee, J. I. Gonzalez, J. Zheng and R. M. Dickson, *Acc. Chem. Res.*, 2005, **38**, 534–541; (*e*) U. Pischel, *Angew. Chem., Int. Ed.*, 2007, **46**, 4026–4040; (*f*) *Molecular Switches*, 2nd ed.; B. L. Feringa, Ed.; Wiley: New York, 2007; (*g*) V. Balzani, A. Credi and M. Venturi, *Molecular Devices and Machines-Concepts and Perspectives for the Nanoworld*, 2nd ed.; Wiley-VCH: Weinheim, 2008; (*h*) I. Yildiz, E. Deniz and F. M. Raymo, *Chem. Soc. Rev.*, 2009, **38**, 1859–1867; (*i*) M. Amelia, L. Zou and A. Credi, *Coord. Chem. Rev.*, 2010, **254**, 2267–2280.

17 (*a*) H. A. Saroff and H. J. Mark, *J. Am. Chem. Soc.*, 1953, **75**, 1420–1426; (*b*) Y. Li, X.-P. Yan, C. Chen, Y.-L. Xia and Y. J. Jiang, *J. Proteome Res.*, 2007, **6**, 2277–2286.

18 A. J. Parola, J. C. Lima, F. Pina, J. Pina, J. Seixas de Melo, C. Soriano, E. Garcia-España, R. Aucejo and J. Alarcon, *Inorg. Chim. Acta*, 2007, **360**, 1200–1208.

19 *Mercury Update: Impact on Fish Advisories*, EPA Fact Sheet EPA-823-F-01-011; EPA, Office of Water, Washington, DC, 2001.

20 (*a*) S. P. Watton, J. G. Wright, F. M. Macdonnell, J. W. Bryson, M. Sabat and T. V. Ohalloran, *J. Am. Chem. Soc.*, 1990, **112**, 2824–2826; (*b*) A. Ono and H. Togashi, *Angew. Chem., Int. Ed.*, 2004, **43**, 4300–4302; (*c*) S. V. Wegner, A. Okesli, P. Chen and C. He, *J. Am. Chem. Soc.*, 2007, **129**, 3474–3475; (*d*) C.-K. Chiang, C.-C. Huang, C.-W. Liu and H. T. Chang, *Anal. Chem.*, 2008, **80**, 3716–3721; (*e*) Z. D. Wang, J. H. Lee and Y. Lu, *Chem. Commun.*, 2008, 6005–6007.

21 E. Cielen, S A. Tobiecka, A. Tahri, G. Hoornaert, F. C. De Schryver, J. Gallay, M. Vincent and N. Boens, *J. Chem. Soc. Perkin Trans.*, 2002, **2**, 1197–1206.

22 R. A. Bissell, A. P. de Silva, H. Q. N. Gunaratne, P. L. M. Lynch, G. E. M. Maguire, C. P. McCoy and K. R. A. S. Sandanayake, *Top. Curr. Chem.*, 1993, **168**, 223–264.

23 H.-W. Li, Y. Li, Y.-Q. Dang, L.-J. Ma, Y. Wu, G. Hou and L. Wu, *Chem. Commun.*, 2009, 4453–4455.

24 S. Aoki, Y. Tomiyama, Y. Kageyama, Y. Yamada, M. Shiro and E. Kimura, *Chem.–Asian J.*, 2009, **4**, 561–573.

25 A. Dhir, V. Bhalla and M. Kumar, *Org. Lett.*, 2008, **10**, 4891–4894.

26 (*a*) A. J. Canty, N. Chaichit, B. M. Gatehouse, E. E. George and G. Hayhurst, *Inorg. Chem.*, 1981, **20**, 2414–2422; (*b*) A. J. Canty, N. Chaichit, B. M. Gatehouse and E. E. George, *Inorg. Chem.*, 1981, **20**, 4293–4300.

27 (*a*) S. H. Whitlow, *Can. J. Chem.*, 1974, **52**, 198–202; (*b*) L. G. Kuz'mina, N. G. Bokii and Yu. T. Struchkow, *Russ. Chem. Rev.*, 1975, **44**, 73–85.

28 (*a*) B. Valeur, *Molecular Fluorescence: Principles and Applications*Wiley-VCH: Weinheim, 2002; (*b*) J. R. Lakowicz, *Principles of Fluorescence Spectroscopy*, 3rd ed.; Kluwer Academics/Plenum Publishers: New York, 2006.

29 G. Schwarzenbach, *Complexometric Titrations*, Chapman and Hall: London, 1957.

30 (*a*) T. Wu, Q. Wu, S. Guan, H. Su and Z. Cai, *Biomacromolecules*, 2007, **8**, 1899–1906; (*b*) R. B. Singh, S. Mahanta, A. Bagchi and N. Guchhait, *Photochem. Photobiol. Sci.*, 2009, **8**, 101–110.

31 Z. R. Grabowski, K. Rotkiewicz and W. Rettig, *Chem. Rev.*, 2003, **103**, 3899–4032.

32 C. T. Lin, H. W. Guan, R. K. McCoy and C. W. Spangler, *J. Phys. Chem.*, 1989, **93**, 39–43.

33 A. K. Bhuyan, *Biochemistry*, 2002, **41**, 13386–13394.

34 A. V. Hill, *J. Physiol.*, 1910, **40**, iv–vii.

35 R. P. Haugland, *Handbook of Fluorescent Probes and Research Chemicals*, 9th ed.; Molecular Probes Inc: Leiden, 2002.

36 In *Geigy Scientific Tables*, 8th ed.; C. Lentner, Ed.; Ciba-Geigy: Basel, 1984; Vol. 3, pp 65.

37 BSA concentrations in serum samples are determined by detecting the absorption of Tyr and Trp at 280 nm, and 1 mg mL^{-1} BSA is set as a protein standard of $A_{280nm} = 0.66$.

38 H. Koyama and T. Yoshino, *Bull. Chem. Soc. Jpn.*, 1972, **45**, 481–484.

39 (*a*) X. M. Zhang , WO Pat., 97/13763, 1997; (*b*) G. E. Kiefer, J. Simon and J. R. Garlich, WO Pat., 94/26754, 1994.

40 H. Lu, S. Zhang, H. Liu, Y. Wang, Z. Shen, C. Liu and X. You, *J. Phys. Chem. A*, 2009, **113**, 14081–14086.

41 M. J. Frisch, G. W. Trucks, H. B. Schlegel, G. E. Scuseria, M. A. Robb, J. R. Cheeseman, V. G. Zakrazewski, J. A. Montgomery Jr., R. E. Startmann, J. C. Burant, S. Dapprich, J. M. Millam, A. D. Daniels, K. N. Kudin, M. C. Strain, O. Farkas, J. Tomasi, V. Barone, M. Cossi, R. Cammi, B. Mennucci, C. Adamo, S. Clifford, J. Ochterski, G. A. Petersson, P. Y. Ayala, Q. Cui, K. Morokuma, D. K. Malik, A. D. Rabuck, K. Raghavachar, J. B. Foresman, J. Cioslowski, J. V. Ortiz, B. B. Stefanov, G. Liu, A. Liashenko, P. Piskorz, I. Komaromi, R. Gomperts, R. L. Martin, D. J. Fox, T. Keith, M. A. Al-Laham, C. Y. Peng, A. Nanyakkara, C. Gonzalez, M. Challacombe, P. M. W. Gill, B. Johnson, W. Chen, M. W. Wong, J. L. Andres, M. Head-Gordon, E. S. Replogle and J. A. Pople, *Gaussian 98*, Revision A.9; Gaussian Inc: Pittsburgh, PA, USA, 1998.